Distribution of this document is unlimited.

FLARE HAZARDS AT SOLAR MINIMUM: DOSIMETRIC EVALUATION OF THE CLASS 2 FLARE OF FEBRUARY 5, 1965

Hermann J. Schaefer

Bureau of Medicine and Surgery
MF022.03.02-5001.35

NASA Order No. R-75

Approved by

Captain Ashton Graybiel, MC USN
Director of Research

Released by

Captain H. C. Hunley, MC USN
Commanding Officer

2 June 1966

U.S. NAVAL AEROSPACE MEDICAL INSTITUTE
U.S. NAVAL AVIATION MEDICAL CENTER
PENSACOLA, FLORIDA

SUMMARY PAGE

THE PROBLEM

The proton flux of the Class 2 flare of February 5, 1965, occurring at midpoint of the Years of the Quiet Sun 1964-65, has been recorded during the two-day period of enhanced radiation intensity by the polar orbit satellite 1964-45A. These data lend themselves to an evaluation of the instantaneous radiation levels and the total flare exposure behind typical shield systems.

FINDINGS

Conversion of the energy spectra for the flare produced proton flux recorded at five different times during the radiation surge furnishes differential range spectra of a steep negative slope with the bulk of particle flux concentrated in the range interval from 0.1 to 1.0 g/cm^2. The corresponding dose distributions for a uniform shield thickness of 0.1 g/cm^2 exhibit a similarly steep depth dose gradient. The half value layers range from 2.6 to 5.6 millimeters of tissue, characterizing the radiation as of very low penetrating power. The dose rate for the highest flux level equals 714 millirads/hour for the tissue surface behind 0.1 g/cm^2 shielding. The corresponding dose rates for the front half-spaces (2 pi) of the Gemini and Apollo shield distributions are 81 and 11 millirads/hour, respectively, demonstrating well the low penetrating power of the flare produced proton beam. The integral flare dose for the tissue surface behind 0.1 g/cm^2 shielding equals 8.3 rads over the 44 hour period of enhanced flux, indicating that the flare event would not have constituted a major hazard for a manned space mission in progress.

INTRODUCTION

On February 5, 1965, almost exactly at midpoint in the two-year period officially designated as the "Years of the Quiet Sun," a Class 2 flare developed on the solar disk and emitted a proton beam into interplanetary space which was recorded, in the vicinity of the Earth, by the radiation sensors of the polar orbit satellite 1964-45A. Paulikas, Freden, and Blake (1) have reported these measurements, establishing the energy spectra of the proton flux in the polar region at five different times during the flare produced radiation surge. Though the limited resolution of kinetic energies and the comparatively large statistical error of the particle counts define the energy spectra only with moderate accuracy, a quantitative evaluation of the data with regard to the dose distribution that would develop in a human target in a space system of a given shield equivalent seems of definite interest.

It should be emphasized from the beginning that the dosages in question would appear to cause concern only for systems of very low shielding such as the Lunar Excursion Module (LEM) or under conditions of Extra Vehicular Activity (EVA). Even for these systems, the integral flare dose remains quite moderate, not fully reaching the 10 rad level for the body surface. Nevertheless, a quantitative assessment of the depth dose distribution for this particular flare event seems of special interest in view of the generally accepted assumption that, during solar minimum, manned space operations are completely safe as far as radiation hazards from solar particle beams are concerned. To be sure, it has been known for a long time that small centers of activity, sometimes leading to minor flares, develop on the Sun also at solar minimum; yet fluxes and energy spectra of the proton beams emitted from these small flares were supposed to be such that, even in space systems of low shielding, the radiation exposure of the astronaut remained on the general level of the galactic radiation.

As will be shown, the flare of February 5, 1965 proves the just-indicated proposition to be essentially wrong. That this is so cannot immediately be seen from the publication of Paulikas and co-workers (l.c., 1), because the flux/energy notation used by the physicist for presenting data on solar particle beams does not allow a simple and direct conversion to absorbed doses in a human target for a given shield thickness. It therefore seems desirable to evaluate the flare data in question explicitly in terms of the depth dose distribution in a tissue phantom or human target. The following brief note is an attempt in this direction. It is limited strictly to this particular aspect. For a discussion of the more general astrophysical implications with regard to flare activity at solar minimum and the state of the interplanetary medium, the reader is referred to the original publication (l.c., 1).

RANGE SPECTRA OF PROTON BEAM AT VARIOUS TIMES

The first step in establishing the depth dose distribution for a given integral or differential energy spectrum is the conversion of the energy spectrum into the range spectrum. The latter spectrum not only lends itself much more easily to computations

of absorbed doses in compact absorbers, but also itself conveys directly an idea of the depth of penetration of the radiation. It therefore seems of interest to present the complete set of differential range spectra as they prevailed at different times of the flare event.

Data on the energy spectrum of the flare produced proton surge are available for five different times: at 2216 Universal Time (UT) on February 5, i.e., about 4 $\frac{1}{2}$ hours after onset of the visible flash of light on the Sun; at 0018 UT, 0022 UT, and 1517 UT on February 6; and at 1800 UT on February 7. In the last of these five spectra, flux levels are so low that the corresponding tissue dosages stay well below the official permissible level. The evaluation of depth dose distributions, therefore, has been limited to the first four spectra. Table I lists the time sequence of flare development and the sampling times at which energy spectra were recorded. The corresponding differential range spectra A to D are shown in Figure 1. Of special interest is the sharp reincrease of flux between 0018 and 0022 UT on February 6. The exact cause for this discontinuous rise of intensity, presumably an outcome of interactions of the quiet day solar wind with the more rapidly moving plasma from the flare is not known. From the dosimetric standpoint, the reincrease of the flux level is of interest inasmuch as it indicates that, in assessing the integral flare dose, the assumption of a smooth time profile for the development and decay of a flare produced radiation surge cannot always be relied upon.

Table I

Sampling Times for Energy Spectrum of Proton Beam from Flare of February 5, 1965

Time	Event	Time after Flash
Feb. 5, 1750 UT	Onset of Visible Flash	
2216	Spectrum A	4 hrs 26 min
Feb. 6, 0018	Spectrum C	6 hrs 28 min
0022	Spectrum B	6 hrs 32 min
1517	Spectrum D	21 hrs 27 min
Feb. 7, 1800	Flux approaches background	48 hrs 10 min

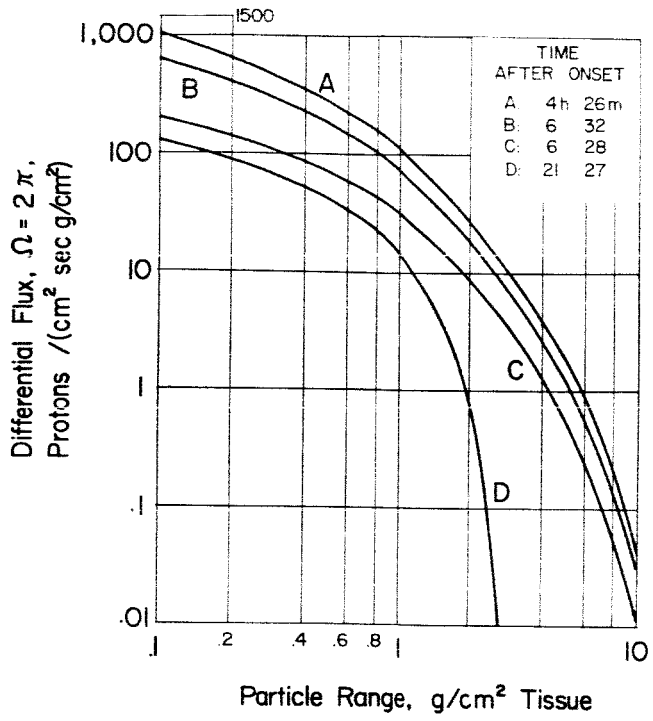

Figure 1

Differential Range Spectra of Solar Proton Beam from February 5, 1965 Flare at High Geomagnetic Latitude at Four Different Times

The basic configuration of the differential range spectra shown in Figure 1 fits well into the general pattern of spectra of large flare events that have occurred during the maximum of the preceding solar cycle in the years 1958 to 1961. As in these earlier events, the spectra exhibit a steep negative slope; i.e., the flux drops steeply for increasing penetrating power. Usually, though remaining negative all the time, the slope of the spectrum shows a marked change in steepness as the flare produced proton surge develops and decays. Since protons of higher energies travel faster in interplanetary space, they arrive and disappear earlier in the vicinity of the Earth during the time of increased flux. As a consequence, the relative abundance of low energy protons should increase with time. The spectra in Figure 1 indicate this trend clearly only for the step from Spectrum C to Spectrum D, i.e., in the terminal phase of the event. It should be realized, however, that data on the spectral configuration for the initial period, where the transition is always especially pronounced, are not available. Furthermore, since the original data on which the spectral configuration is based distinguish only three energy bands, the possibilities of recognizing a slowly progressing change of slope from spectrum to spectrum are limited.

DEPTH DOSE DISTRIBUTION

The differential range spectra in Figure 1 show that the bulk of the flux at all times during the flare event is concentrated in the range interval from 0.1 to 1 g/cm^2. For Spectrum A, for instance, the differential flux drops by a factor of 10 in proceeding from the 0.1 to 1 g/cm^2 range. This indicates that an analysis of the depth dose distribution is of interest mainly for systems of very low shielding (LEM, EVA) and that, regardless of shielding, the highest exposure always will occur in near-surface regions of the target behind the shielding. For a human body as target, then, the dose will be highest in the skin and subcutaneous tissue. Considering the size of the human body, one can easily see that the exposure in the surface, because of the low penetrating power of the radiation, is predominantly due to particles arriving within a limited solid angle about the vertical direction on the body surface. For incidence at oblique or grazing angles and, even more, from the opposite side of the body, the pathways in shield material and tissue are long. Therefore, only the low fluxes of particles of higher ranges in the spectrum can penetrate to the point of exposure. That means the exposure geometry is very satisfactorily approximated by a semi-infinite slab behind a plane shield irradiated by a particle stream arriving from all directions of the front half-space (2 pi incidence).

The computational analysis of the depth dose distributions for the just-described system was carried out by numerical methods using the computer code used in an earlier study of other flare events (2). The results are compiled in Figure 2 showing the depth dose distributions for the four spectra of Figure 1. Since a depth in tissue of zero (body surface) cannot be indicated on a logarithmic scale, the abscissa values in Figure 2 show depth in tissue combined with shield thickness. In other words, the dose rate in the body surface is plotted at 0.1 g/cm^2. This plotting of the combined depth in tissue and shield thickness facilitates at the same time the reading of surface dose rates for any other shield thickness that might be of interest.

In conventional radiation therapy the penetrating power of a beam usually is denoted by the half value layer (HVL). The progressive changes in penetrating power that occur as the beam penetrates more deeply into the body can be described, in this notation, by the first, second, and third HVL's. For the four spectra of the flare event under discussion shown in Figure 1, the first three HVL's are compiled in Table II. To be sure, these values are not derived from the depth dose distributions in Figure 2, but have been established by a separate calculation for the geometry of a parallel beam of right-angle incidence. It is seen from Table II that the HVL's for the radiation under investigation are considerably smaller than those encountered in conventional x-ray therapy which usually range from about 1 to 10 centimeters of tissue. On the other hand, the HVL's in Table II do not qualify the radiation as "of extremely low penetrating power" in terms of the official definition of the National Committee on Radiation Protection (3) which sets the HVL for such radiations at "less than 1 millimeter of soft tissue."

Table II

Half Value Layers (HVL) in Millimeter Tissue for Proton Beam of February 5, 1965 Flare at Various Times

Spectrum	Time after Onset	1st HVL	2nd HVL	3rd HVL
A	4 hrs 26 min	2.6	4.0	4.6
B	6 hrs 32 min	2.8	3.9	5.0
C	6 hrs 28 min	3.3	5.1	5.6
D	21 hrs 27 min	2.7	3.3	2.8

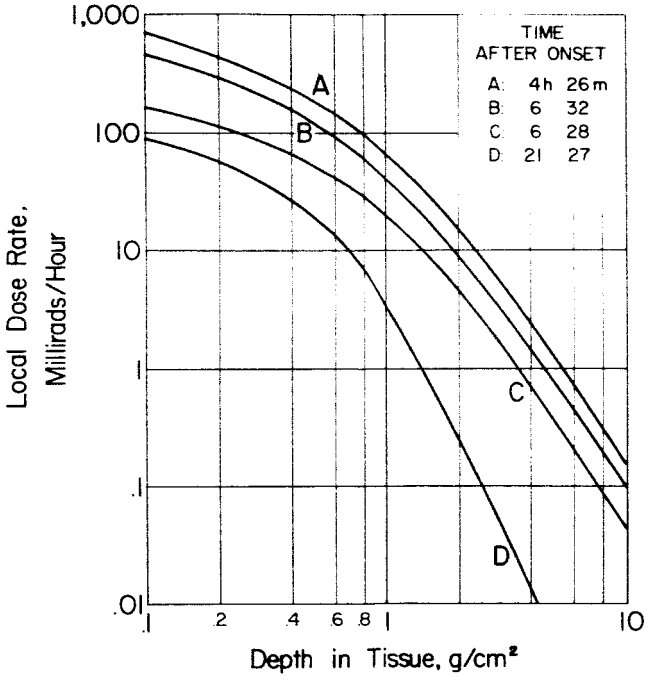

Figure 2

Depth Dose Distributions in Semi-Infinite Tissue Slab for Four Spectra Shown in Figure 1

The data in Table II indicate a considerable increase of consecutive HVL's for the same spectrum with exception of Spectrum D. This hardening of the beam as it penetrates more deeply is a well-known phenomenon in conventional radiation therapy. It is caused by the stronger absorption of beam components of lower penetrating power, or, in terms of the flare produced proton beam, by the selective elimination of particles of lower ranges.

A comparison of HVL's of the same order for different spectra reveals a slight increase of the HVL from Spectrum A to Spectrum C, followed by a marked decrease in Spectrum D. This slight increase is actually not in agreement with the transition usually found in flare events as they progress in time. Since, as pointed out in the preceding section, high energy particles arrive first in the vicinity of the Earth, the penetrating power of the beam, i.e., its HVL, usually is higher early in the event. This trend is correctly indicated only in the transition from Spectrum C to D. Here again, however, a full clarification of the issue would require data during the initial phase of the event, which just are not available.

Aside from the incomplete picture concerning the change of HVL's with time, the finding of generally very small HVL's is in agreement with recordings of flare beams in general. It points to the basic difficulties that arise if the true radiation injury is to be determined that would result from total body exposure with such steeply dropping depth dose distributions. These aspects have been discussed repeatedly (4) and shall not be subjected to further examination here.

TIME PROFILE OF EXPOSURE: THE INTEGRAL FLARE DOSE

For a complete dosimetric evaluation, the analysis of instantaneous dose rates with their depth dose distributions at selected times during the flare produced radiation surge has to be supplemented by the determination of the total exposure accumulated during the entire time span of increased flux. For this purpose the full time profile of the radiation level during the development and decay of the radiation surge must be known. In this respect the data on the flare event under discussion are incomplete. As can be seen from Table I, the energy spectrum has been sampled only five times over a time interval of forty-eight hours from the onset of the visible flash on the Sun to the point where the radiation level in the vicinity of the Earth dropped to an insignificant level. Of these five measurements, the first one was taken $4\frac{1}{2}$ hours after onset of the flare. High energy protons usually start arriving at the Earth some fifteen minutes after onset of the visible flash; thus, the flux during the first four hours after the flare remains undetermined. This is especially unfortunate because, very likely, the maximum of the proton surge occurred during this time. Further restricting inferences on the time profile is the fact that Spectra B and C show a large discontinuous reincrease of the radiation level, leaving it an open question which of the two spectra should be considered as representative for the average flux level at the time these two spectra were observed. Finally, the fourth spectrum, D, showing a very small flux level, merely marks the approaching end of the event without actually contributing information on the time profile as such.

It is seen, then, that a reliable time profile just cannot be established. If one would want to indulge in speculation, drawing an arbitrary time profile through the few points available, the upper graph of Figure 3 could be offered as a possible assumption. It connects the instantaneous skin dose rates for Spectra A, B, and D, disregarding Spectrum C entirely, and makes a conservatively low estimate of the time course for the initial radiation surge between zero hour and Spectrum A.

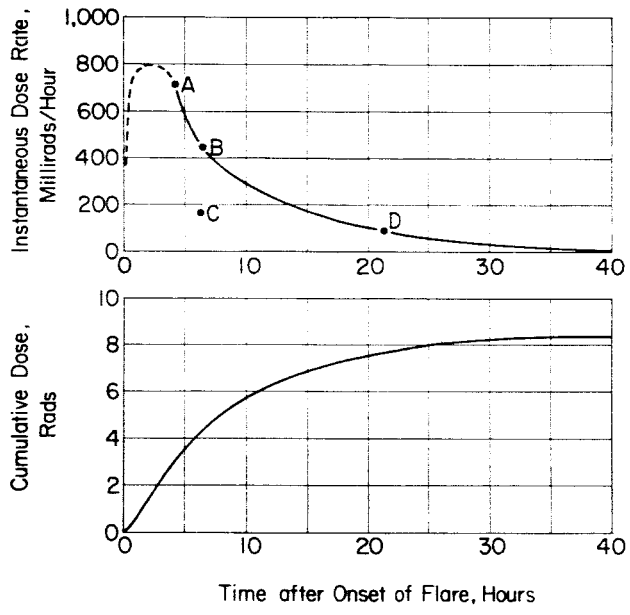

Figure 3

Conception of Time Profile of Radiation Exposure for February 5, 1965 Flare

Top: Dose rate in surface of tissue slab behind 0.1 g/cm^2 shielding.
Bottom: Cumulative dose.

Numerical integration of the time profile in Figure 3 leads to a total skin dose of 8.3 rads accumulated in the time from zero to forty-eight hours. The time profile of accumulation of this dose is shown in the lower graph of Figure 3. It follows the basic pattern seen in all flare events. The exposure grows comparatively fast in the first few hours and then very gradually levels off at its terminal value as the flare produced flux slowly drops to insignificant levels. As pointed out before, the estimate of the initial section of the time profile from zero to 4 $\frac{1}{2}$ hours is conservatively low as most flares show a more sharply peaked and higher maximum in the first few hours after onset than the one assumed in Figure 3. Therefore, the integral flare dose of 8.3 rads for the body surface behind 0.1 g/cm^2 shielding constitutes a low estimate. On the other hand, as seen from Figure 3, the estimated initial time profile accounts for only 40 per cent of

the integral flare dose with the balance of 60 per cent spread over the much longer time span of almost forty-four hours. Since this latter part of the curve is smoothly fitted to three observed values, the larger part of the integral flare dose seems reliably established. Disregarding Spectrum C seems justified on the plausible assumption that it represents an abnormally low flux level caused by short-term field fluctuations in the outer magnetosphere.

FLARE EXPOSURE FOR GEMINI AND APOLLO SHIELD DISTRIBUTIONS

The forgoing analysis has demonstrated that, for the flare event under investigation, significant exposure levels occur only in systems of very low shielding. It seems nevertheless of interest to add, to the data for a tissue slab behind a uniform shield of 0.1 g/cm^2, at least sample values for the complex shield distributions of actual space systems. Very elaborate analyses of such distributions have been carried out for the Gemini spacecraft (5) and for the combined Command and Service Module of the Apollo spacecraft (6). In view of the limited accuracy of the flux data available for the flare event under investigation, an estimate of the highest radiation level, i.e., for Spectrum A, seems sufficient. Furthermore, the computational analysis is greatly simplified if only the so-called exposure dose ("air dose" in the older terminology) is evaluated, i.e., the dose as it would develop in a very small tissue sample inside the shield system at the point of interest, since no self-shielding has to be considered. However, the exposure dose can still be considered as closely representative of the highest skin dose, which occurs at a point of the body for which a free "line of sight" exists to the solid angles with the lowest shield thicknesses. This is so because at that particular location the bulk of the exposure is due to the fluxes through the lowest shield thicknesses which are not influenced by self-shielding.

As mentioned before, the two shield distributions in question are very detailed. For the full tabulations, the reader should consult the original publications (l.c., 5 and 6). The computational evaluation has been carried out using these original tabulations. The Apollo shield system (l.c., 6) is subdivided, in the original study, into the anterior and the posterior 2 pi half-spaces as seen from the center astronaut in the Command Module. Only the anterior of these two half-spaces has been evaluated since it contains substantially lower shield thicknesses throughout. The posterior distribution covers the heavy heat shield and, in the Service Module, two large fuel tanks, a rocket engine, and other heavy equipment affording enormous shielding equivalents up to 212 g/cm^2.

A division into the anterior and posterior half-space is not available for the Gemini shield distribution (l.c., 5). However, there, as in the Apollo spacecraft, low shield thicknesses center strongly on the anterior side, i.e., on the front side of the astronauts, whereas the heavy heat shield covers most of the posterior side. Therefore, the evaluation of the exposure level was carried out for a solid angle of 2 pi, containing the lower half of the full distribution.

Tables III and IV show the two shield systems and the corresponding fractional dose rate contributions for Spectrum A. The distributions in the tables have been simplified by lumping together, in the range of medium high and high shield thicknesses, several fractional solid angles into one. However, the contributions to exposure were computed by using the fully itemized original tabulations. Total dose rates are listed at the bottom of the dose rate column in either table. As was to be expected from the steep negative slope of the range spectrum, these total dose rates, 81 millirads/hour for the Gemini and 11 millirads/hour for the Apollo system, are substantially lower than the dose rate of 714 millirads/hour for the uniform plane shield of 0.1 g/cm^2. It is interesting to note that, for the Apollo vehicle, 90 per cent of the exposure is due to the large solid angle No. 2 with the low mean thickness of 1.81 g/cm^2. No single solid angle that contributed practically the full dose rate could be pointed out for the Gemini distribution. However, as can be seen from Table III, also in this case the bulk of exposure is concentrated in a few angles of low shield thicknesses.

DISCUSSION

From the viewpoint of manned space operations, the main significance of the data reported by Paulikas and co-workers and evaluation of those data in terms of tissue dosages presented in this study rests in the fact that reliable quantitative information now seems established on radiation levels and penetrating powers of a solar particle beam for a flare event at solar minimum. As far as satellite observations during the Years of the Quiet Sun allow conclusions, the flare event of February 5, 1965 was the largest of the entire period and, for that matter, the only one that would have produced significant radiation levels behind 0.1 g/cm^2 shielding. On the one hand, this finding is reassuring because an integral flare dose of 8 rads for systems of very low shielding and the substantially lower doses for the Gemini and Apollo shield systems would not seem to affect a space mission in progress in any way. On the other hand, the findings obviously indicate that precautionary measures of flare surveillance are called for even during the minimum of the solar cycle.

From the radiobiological and dosimetric viewpoint, the finding of a steeply dropping depth dose distribution for the flare beam under investigation is nothing new. It poses a number of questions with regard to the true radiation damage that such peculiar dosage fields in the body would produce and with regard to the definition of permissible exposure. Since these aspects have been discussed repeatedly (7), no further comments seem necessary here.

Table III

Shield Distribution of Gemini Spacecraft*

Solid Angle, No.	Solid Angle, sterad	Thickness Interval, g/cm^2	Dose Rate, Spectrum A, mr/hr
1	0.0698	0.195 - 0.293	8.93
2	0.0175	0.293 - 0.391	1.76
3	0.0349	0.391 - 0.488	1.42
4	0.0175	0.488 - 0.586	1.18
5	0.0524	0.586 - 0.684	2.95
6	0.4189	0.684 - 0.879	19.58
7	0.2618	0.879 - 1.07	8.33
8	0.5061	1.07 - 1.27	12.25
9	0.3840	1.27 - 1.47	7.45
10	0.2618	1.47 - 1.66	3.89
11	0.4887	1.66 - 2.05	5.11
12	0.2793	2.05 - 2.44	2.05
13	0.3142	2.44 - 2.83	1.51
14	0.1572	2.83 - 3.22	0.55
15	0.9076	3.22 - 4.00	1.86
16	0.8029	4.00 - 4.79	1.10
17	0.5412	4.79 - 6.15	0.36
18	0.7681	6.15 - 7.71	0.23
TOTAL:	6.2839		80.51

*Shown are the intervals of lowest thicknesses that make up a total angle of 2 pi steradians in order to obtain a conservatively high estimate of the radiation level for 2 pi incidence. Beginning with solid angle No. 6, each entry is the sum of 2 intervals of the original tabulation, with No. 11, of 4, and with No. 15, of 8. Thicknesses shown are slant thicknesses as seen from center of astronauts' seats. No self-shielding considered.

Table IV

Shield Distribution of Apollo Spacecraft*

Solid Angle, No.	Solid Angle, sterad	Mean Thickness, g/cm^2	Dose Rate, Spectrum A, mr/hr
1	0.0171	1.68	0.21
2	0.9380	1.81	10.05
3	0.1105	3.6	0.22
4	0.0239	4.1	0.04
5	0.0190	4.2	0.03
6	0.0912	5.0	0.07
7	0.0665	5.7	0.03
8	0.1624	7.1	0.04
9	0.4083	7.5	0.09
10	0.9312	8.5	0.14
11	0.1066	9.7	0.01
12	0.5256	10.6	0.05
13	0.3323	11.0	0.03
14	0.2758	13.0	0.02
15	0.4470	13.9	0.03
16	0.3865	15.6	0.02
17	0.1230	17.7	0.07
18	0.3623	22.0	0.02
19	0.9536	28.0	0.04
TOTAL:	6.2808		11.16

*Shown are the solid angles on the anterior side as seen from the astronauts for the combined Command and Service Module. Thicknesses are mean slant thicknesses as seen from the center astronaut's seat. No self-shielding considered.

REFERENCES

1. Paulikas, G. A., Freden, S. C., and Blake, J. B., Solar proton event of February 5, 1965. J. Geophys. Res., 71:1795-1798, 1966.

2. Schaefer, H. J., A note on the dosimetric interpretation of rigidity spectra for solar particle beams. NAMI-960. NASA Order R-75. Pensacola, Fla.: Naval Aerospace Medical Institute, 1966.

3. Permissible dose from external sources of ionizing radiation. Handbook 59. Washington, D. C.: National Bureau of Standards, 1954.

4. Schaefer, H. J., Radiation exposure in solar particle beams behind very low shielding. NSAM-914. NASA Order R-75. Pensacola, Fla.: Naval School of Aviation Medicine, 1965.

5. Chappell, D. A., Kloster, R. L., and Warneke, C. H., Inherent shielding and dose rate calculations for Gemini spacecraft. St. Louis, Mo.: McDonnell Aircraft Corporation, 1964.

6. Schaefer, H. J., Dosimetric evaluation of data on the solid angle breakdown of shield thickness for the Apollo vehicle. NSAM-903. NASA Order R-75. Pensacola, Fla.: Naval School of Aviation Medicine, 1964.

7. Radiation Biology and Space Environmental Parameters in Manned Spacecraft Design and Operations. A Special Report. Aerospace Med., 36: No. 2—Section II, 1965.

Security Classification

UNCLASSIFIED **DOCUMENT CONTROL DATA - R&D**

(Security classification of title, body of abstract and indexing annotation must be entered when the overall report is classified)

1. ORIGINATING ACTIVITY (Corporate author)
U.S. Naval Aerospace Medical Institute
Pensacola, Florida

2a. REPORT SECURITY CLASSIFICATION
Unclassified

2b. GROUP

3. REPORT TITLE
FLARE HAZARDS AT SOLAR MINIMUM: DOSIMETRIC EVALUATION OF THE CLASS 2 FLARE OF FEBRUARY 5, 1965

4. DESCRIPTIVE NOTES (Type of report and inclusive dates)

5. AUTHOR(S) (Last name, first name, initial)
Schaefer, Hermann J.

6. REPORT DATE	7a. TOTAL NO. OF PAGES	7b. NO. OF REFS
2 June 1966	13	7

8a. CONTRACT OR GRANT NO. NASA R-75	9a. ORIGINATOR'S REPORT NUMBER(S)
b. PROJECT NO. MF022.03.02-5001	NAMI-970
c.	9b. OTHER REPORT NO(S) (Any other numbers that may be assigned this report)
d.	35

10. AVAILABILITY/LIMITATION NOTICES Qualified requesters may obtain copies of this report from DDC. Available, for sale to the public, from the Clearinghouse for Federal Scientific and Technical Information, Springfield, Virginia 22151.

11. SUPPLEMENTARY NOTES	12. SPONSORING MILITARY ACTIVITY

13. ABSTRACT

The proton energy spectra for the Class 2 solar flare of February 5, 1965, as reported by a polar orbit satellite at five different times during the two-day period of enhanced intensity, are evaluated in terms of tissue depth doses for a semi-infinite slab with 0.1 g/cm^2 shielding and for the Gemini and Apollo shield distribution. Maximum dose rates for the tissue surface are 714 millirads/hour, 81 and 11 millirads/hour, respectively. For the unidirectional beams, half value layers range from 2.6 to 5.6 millimeters of tissue. The integral flare dose over forty-four hours is 8.3 rads for the tissue surface behind 0.1 g/cm^2 shielding.

DD FORM 1 JAN 64 1473

UNCLASSIFIED

Security Classification

Security Classification

14. KEY WORDS	LINK A		LINK B		LINK C	
	ROLE	WT	ROLE	WT	ROLE	WT
UNCLASSIFIED Radiation hazards in space Flare produced proton beams at solar minimum Tissue half value layers for solar protons Flare exposure behind various shield systems						

INSTRUCTIONS

1. ORIGINATING ACTIVITY: Enter the name and address of the contractor, subcontractor, grantee, Department of Defense activity or other organization *(corporate author)* issuing the report.

2a. REPORT SECURITY CLASSIFICATION: Enter the overall security classification of the report. Indicate whether "Restricted Data" is included. Marking is to be in accordance with appropriate security regulations.

2b. GROUP: Automatic downgrading is specified in DoD Directive 5200.10 and Armed Forces Industrial Manual. Enter the group number. Also, when applicable, show that optional markings have been used for Group 3 and Group 4 as authorized.

3. REPORT TITLE: Enter the complete report title in all capital letters. Titles in all cases should be unclassified. If a meaningful title cannot be selected without classification, show title classification in all capitals in parenthesis immediately following the title.

4. DESCRIPTIVE NOTES: If appropriate, enter the type of report, e.g., interim, progress, summary, annual, or final. Give the inclusive dates when a specific reporting period is covered.

5. AUTHOR(S): Enter the name(s) of author(s) as shown on or in the report. Enter last name, first name, middle initial. If military, show rank and branch of service. The name of the principal author is an absolute minimum requirement.

6. REPORT DATE: Enter the date of the report as day, month, year; or month, year. If more than one date appears on the report, use date of publication.

7a. TOTAL NUMBER OF PAGES: The total page count should follow normal pagination procedures, i.e., enter the number of pages containing information.

7b. NUMBER OF REFERENCES: Enter the total number of references cited in the report.

8a. CONTRACT OR GRANT NUMBER: If appropriate, enter the applicable number of the contract or grant under which the report was written.

8b, 8c, & 8d. PROJECT NUMBER: Enter the appropriate military department identification, such as project number, subproject number, system numbers, task number, etc.

9a. ORIGINATOR'S REPORT NUMBER(S): Enter the official report number by which the document will be identified and controlled by the originating activity. This number must be unique to this report.

9b. OTHER REPORT NUMBER(S): If the report has been assigned any other report numbers *(either by the originator or by the sponsor)*, also enter this number(s).

10. AVAILABILITY/LIMITATION NOTICES: Enter any limitations on further dissemination of the report, other than those imposed by security classification, using standard statements such as:

(1) "Qualified requesters may obtain copies of this report from DDC."

(2) "Foreign announcement and dissemination of this report by DDC is not authorized."

(3) "U. S. Government agencies may obtain copies of this report directly from DDC. Other qualified DDC users shall request through _____."

(4) "U. S. military agencies may obtain copies of this report directly from DDC. Other qualified users shall request through _____."

(5) "All distribution of this report is controlled. Qualified DDC users shall request through _____."

If the report has been furnished to the Office of Technical Services, Department of Commerce, for sale to the public, indicate this fact and enter the price, if known.

11. SUPPLEMENTARY NOTES: Use for additional explanatory notes.

12. SPONSORING MILITARY ACTIVITY: Enter the name of the departmental project office or laboratory sponsoring *(paying for)* the research and development. Include address.

13. ABSTRACT: Enter an abstract giving a brief and factual summary of the document indicative of the report, even though it may also appear elsewhere in the body of the technical report. If additional space is required, a continuation sheet shall be attached.

It is highly desirable that the abstract of classified reports be unclassified. Each paragraph of the abstract shall end with an indication of the military security classification of the information in the paragraph, represented as *(TS)*, *(S)*, *(C)*, or *(U)*.

There is no limitation on the length of the abstract. However, the suggested length is from 150 to 225 words.

14. KEY WORDS: Key words are technically meaningful terms or short phrases that characterize a report and may be used as index entries for cataloging the report. Key words must be selected so that no security classification is required. Identifiers, such as equipment model designation, trade name, military project code name, geographic location, may be used as key words but will be followed by an indication of technical context. The assignment of links, roles, and weights is optional.